

# Muon Tomography Algorithms for Nuclear Threat Detection

Richard Hoch<sup>1</sup>, Debasis Mitra<sup>1</sup>, Kondo Gnanvo<sup>2</sup>, and Marcus Hohlmann<sup>2</sup>

<sup>1</sup>Department of Computer Science & <sup>2</sup>Department of Physics and Space Sciences  
Florida Institute of Technology, Melbourne, Florida, USA  
dmitra@cs.fit.edu, {rhoch, hohlmann, kgnanvo}@fit.edu

**Abstract.** In this article on *Muon Tomography* we report our work on the development of an intelligent pattern detection system for materials with high atomic numbers ( $Z$ ) for Homeland Security application. Muons are naturally produced in the upper atmosphere by primary cosmic rays and are used as passive probes of a cargo volume. By sensing the incoming and outgoing tracks and measuring the momentum of each muon for a probed volume one may derive the scattering parameters. A statistical algorithm is being used to estimate scattering densities of the material in each unit volume (voxel) of the probed volume. The article describes the algorithm and some results from our simulation experiments.

## 1. Introduction

Nuclear materials that pose a homeland security threat typically have high atomic numbers ( $Z > 82$ ). It is of vital importance to develop smart, efficient, and inexpensive systems to detect such high- $Z$  materials without opening a container.

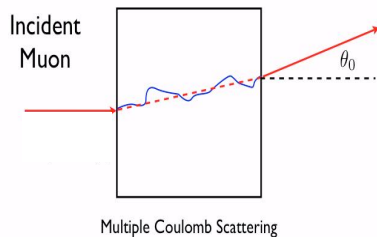


**Fig. 1.** Scattering of a particle

Muons are produced by primary cosmic rays at the upper atmosphere provide an excellent source as passive probes for discriminating materials with different  $Z$ , without extra radiation or incurring any extra cost for the probe generation. Highly penetrating muon tracks may suffer from multiple scatterings by Coulomb interaction with nuclei of atoms on its path. The amount of scattering

depends on the charge  $Z$  of the corresponding nucleus [3] (Fig. 1). The incoming and outgoing tracks for each muon may be detected by appropriate sensors. In our simulations,  $z$ -axis is the vertical direction,  $x$ -axis is the axial direction (cargo movement), and  $y$ -axis is perpendicular to  $xz$ -plane. Sensor arrays parallel to the  $xy$ -plane (typically three) are deployed above and below the probed volume.

## 2. Reconstruction Algorithms

Our first algorithm for reconstruction of scattering points makes a naïve assumption: each scattering is a single event, or only one atomic nucleus (a point) is involved in

scattering. This *Point-of-closest-approach* is called the POCA point [6]. We assign the scattering angle to that point instead of distributing it to multiple points on a muon track as would be the case in multiple scattering. This is a purely geometric algorithm that ignores any underlying physics of scattering. The corresponding *POCA-algorithm* is shown in Fig. 2.

First, the lines corresponding to incoming and outgoing tracks are computed from the corresponding three sensor points where the muons are detected above and below the probed volume, respectively (three sensor-array planes above and three below). We presume that the sensor-electronics will be able to associate the muon detection points to a single muon path by using the timing information of muon detections on the sensor arrays.

In 3D, the incoming and the outgoing tracks are not necessarily coplanar due to scattering and measurement errors, and they are unlikely to meet at a single point. Consequently, for each line (incoming or exiting) the point closest to the

other line is computed using a linear algebraic formulation. The mid-point to these two points is the POCA-point corresponding to each muon (Fig. 3). Also the scattering angle for each muon is computed in line 5. POCA-point and scattering angle pairs are returned for all muons where the angle is not very close to zero (POCA point does not exist for parallel lines or where a muon has traversed without any scattering). Complexity of POCA is  $O(M)$  for  $M$  tracks.

The POCA algorithm is a simple algorithm with a very strong assumption of single-point scattering. A better algorithm, originally proposed by Verdi et al. [7], and subsequently adapted by Schultz et al. [5] utilizes both the scattering angle and the measured linear displacement of a muon-track over the  $xy$ -plane [Fig. 3]. Actually, the scattering angle has a near normal distribution that depends on the material and distance of traversal within the material [Eq. 1]. Our next algorithm, Expectation Maximization (*EM*)-*reconstruction*, uses both the information – scattering angles and linear deviations as input. Here, the scattering angle  $\theta_i$  is measured between the incoming and outgoing track-vectors of a muon. The linear deviation  $\delta_i$  is measured

<i>Algorithm POCA</i>
<p><i>Input:</i> A list of {for each muon <math>i</math>, three incoming sensor points <math>(a_i, b_i, c_i)</math> where the muon is detected, and three corresponding exiting sensor points <math>(d_i, e_i, f_i)</math>}</p> <p><i>Output:</i> Corresponding list of {for each muon <math>i</math>, point of closest approach <math>P_i</math> between each incoming and respective exiting tracks, and the scattering angle <math>\theta_i</math> at that point}</p>
<ol style="list-style-type: none"> <li>(1) for each muon <math>i=1</math> to <math>M</math> in the list</li> <li>(2) create incoming track <math>I_i</math>, and exiting track <math>E_i</math> by least-square-fitting the respective three points each</li> <li>(3) using analytical formula, find closest pts <math>s_i</math> and <math>t_i</math>, respectively, on <math>I_i</math> &amp; <math>E_i</math></li> <li>(4) compute mid-pt <math>P_i</math> between <math>s_i</math> &amp; <math>t_i</math></li> <li>(5) compute angle <math>\theta_i</math> between lines <math>I_i</math> &amp; <math>E_i</math></li> <li>(6) return the list of <math>\{(P_i, \theta_i) \mid 1 \leq i \leq M\}</math></li> </ol>
<p><b>Fig. 2.</b> <i>The POCA Algorithm</i></p>

between the point  $E$  representing the actual emergent track at the topmost bottom detector plane and the point  $F$  where the projected-incoming track hits the same horizontal plane of  $E$  (Fig. 3). We use the two  $x$  and  $y$  components for each of the two parameters  $(\theta, \delta_i)$  that improves the chance of determining scattering location by adding extra information. The *EM-reconstruction* algorithm (Fig. 4) attempts to distribute the scattering location along the POCA-track instead of assigning the scattering event to a single point as the *POCA* algorithm does. The track of a muon connects a representative entering point to the POCA point and then the POCA point to a representative exiting point (typically the detection point on the respective nearest sensor- array plane to the volume).

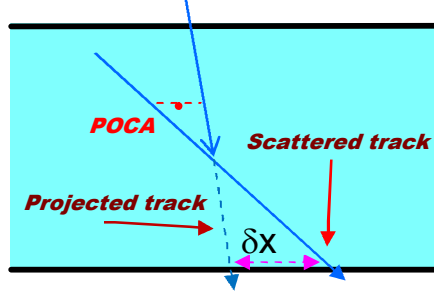


Fig. 3. Linear deviation of a track

This algorithm views a discretized volume for the interrogated space. Each unit of volume is called a voxel and its dimension is predetermined. Scattering is presumed to have happened over some voxels along the POCA track of the muon. The conditional probability (likelihood) of the observed data  $D_i \equiv (\theta_i, \delta_i)$  for a muon  $i$ , given the scattering density distribution  $\lambda$  (a vector) over the voxels ( $j$ ) is given by equation (1).

$$P(D_i | \lambda) = \frac{1}{2\pi^{|\Sigma_i|} |\Sigma_i|^{1/2}} \exp\left(-\frac{1}{2} D_i^T \Sigma_i^{-1} D_i\right) \text{ with } \Sigma_i = p_i^2 \sum_{j=1}^n \lambda_j W_{ij} \quad (1)$$

where the sum is taken over all  $n$  voxels along the  $i$ -th muon track,  $p_i$  is the momentum ratio inversely proportional to momentum  $p_i$ ,  $\lambda_j$  is the scattering density of the  $j$ -th voxel, and  $W$  is the symmetric  $2 \times 2$  covariance matrix between scattering angle  $\theta$  and linear deviation  $\delta$ . Elements of  $W$  depend on the path length of muon  $i$  through voxel  $j$ , and the vertical height of the voxel  $j$  from the bottom plane [5].

Maximizing the total likelihood of observation  $D$ , (by equating a partial derivative of the total log-likelihood with respect to  $\lambda$  to zero, under an assumption of independence between voxels), we get the update equation for the scattering density

$$\lambda_j^{k+1} = \lambda_j^k + \left(\lambda_j^k\right)^2 \text{ median}\left[\left(C_{ij}^k = D_i^T \Sigma_i^{-1} W_{ij} \Sigma_i^{-1} D_i - \text{Trace}(\Sigma_i^{-1} W_{ij})\right)\right], \quad (2)$$

where the median is taken over all tracks  $i$  that go through voxel  $j$ , and  $k$  indicates the iteration index. Asymptotic complexity of the *EM-reconstruction* is  $O(IMN)$ , where  $I$  is the number of iterations,  $M$  is the number of muons, and  $N$  is the number of voxels, and the memory requirement is  $O(M+N)$ .

### 3. Simulation Experiments

GEANT4 [1], a common stochastic physics toolkit for simulating the passage of subatomic particles through material, is used for our experimental set up.

For generating cosmic ray muons we have used a package called CRY, developed at Lawrence Livermore National Lab [8, 10].

The geometry of our standard simple scenario that is used for testing has a probed area with the dimensions 4mX4m in X and Y and 3m in Z. The rectangular targets of five different materials are centered as following: Aluminum at (-1000mm, -1000mm, 0mm), Iron at (1000mm, -1000mm, 0mm), Lead at (0mm, 0mm, 0mm), Tungsten at (-1000mm, 1000mm, 0mm), and Uranium at (1000mm, 1000mm, 0mm). Each of these boxes is of size 40cm×40cm×20cm.

<p><i>Algorithm EM-reconstruction</i></p> <p><i>Input:</i> A list {for each muon <math>i</math>, <math>(D_i, p_{ri})</math>, where <math>D_i = (\theta_i, \delta_i)</math>} &amp; <math>\theta_i</math> is the scattering angle, <math>\delta_i</math> is the displacement of the track, and <math>p_{ri}</math> is the muon momentum parameter; Initial <math>\lambda_j</math>-value for each voxel; Maximum number of iterations <math>I</math>; <i>Output:</i> <math>\lambda_j</math>-value for each voxel</p> <ol style="list-style-type: none"> <li>(1) set initial vector <math>\lambda^{new}</math></li> <li>(2) for each iteration <math>k = 1</math> to <math>I</math> do</li> <li>(3) set vector <math>\lambda^{old} = \lambda^{new}</math></li> <li>(4) for each muon-track <math>i = 1</math> to <math>M</math> do</li> <li>(5) compute <math>C_{ij}</math>, using eq. (2)</li> <li>(6) for each voxel <math>j = 1</math> to <math>N</math> do</li> <li>(7) find median of correction term <math>\Delta\lambda_j</math></li> <li>(8) <math>\lambda_j^{new} = \lambda_j^{old} + \Delta\lambda_j</math>, using eq. 3</li> <li>(9) return vector <math>\lambda</math></li> </ol>
<p><b>Fig. 4.</b> The expectation maximization algorithm</p>

#### 4. Implementation and Results

For reconstruction, we have run the *POCA* algorithm first, which returns a set of *POCA* points and scattering angles at each point. In Fig. 5, the color of a point may indicate the value of the angle assigned to the scattering event at that point.

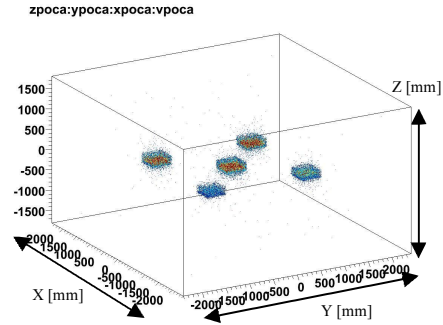


**Fig. 5.** *POCA* reconstruction

We run the *EM-reconstruction* algorithm on the same simulation data after appropriate pre-processing of the input. One of the major challenges in implementing the algorithm is the median calculation for the correction factor of  $\lambda_j$  for each voxel in each iteration. Typically, each such computation requires  $O(H)$  amount of memory (and steps), where  $H$  is the number of tracks through the voxel. This blows up the resource requirement to an impractical level. In order to avoid this we have developed an approximate technique for the median calculation.

The total range of the  $\lambda$ -correction factor is divided into bins of fixed sizes  $d$ . For each bin, the number of data points in the bin and the mean value over the bin is stored which reduces the requirement of storing all data points. Subsequently, the frequency parameters on the binned data points are used to find the median bin and the corresponding mean of that bin is used as the median of the whole data set. The complexity for this computation (for each voxel in each iteration) is  $O(K)$ , where  $K$  is the number of bins, which is far smaller than  $H$ . The error incurred in this

approximation is less than the bin size  $d$ . The smaller  $d$  the better the accuracy is, but a smaller value of  $d$  will increase the value of  $K$  and will consequently decrease computation time and increase memory consumption. To the best of our knowledge this approximate median calculation is new.

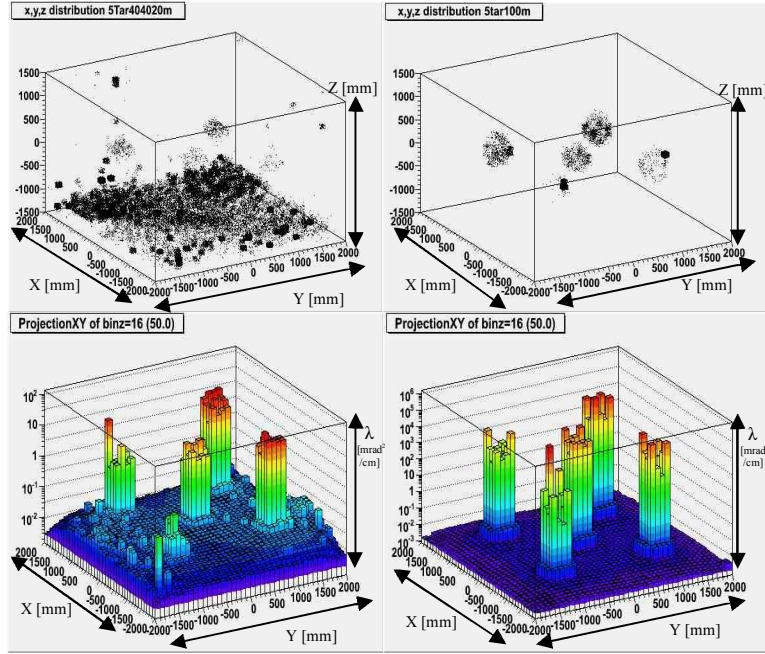


**Fig. 6.** Reconstruction from Expectation Maximization algorithm (average method left; approximate median method right). The top figures are a 3D representation of the  $\lambda$ -values of each voxel. The bottom figures represent  $\lambda$ -values in the plane  $z=50\text{mm}$ .

The result from the *EM-reconstruction* algorithm for the experimental setup discussed in the previous section is shown in Fig. 6. Note that here the output is a voxel-wise  $\lambda$  value, an important difference from Fig. 5. The top plots in Fig. 6 are 3D representations of the  $\lambda$  value for each voxel. Statistically more accurate method is to use average in eq. 2 but median provides better result. The results from the average method are shown on the left. The targets in this plot are barely visible and there is much noise at the bottom of the volume. With the median method shown on the right the reconstruction is much clearer. The targets are clearly visible (though the box shape is distorted) and there is no noise at the bottom. However, the plots at the bottom of Fig. 6, which show the  $\lambda$  values of the voxels in the plane  $z=50\text{mm}$ , indicate that there are still improvements to be made. Both methods discriminate between the targets and the surrounding vacuum, yet for the average method the absolute  $\lambda$  values appear too low and for the median method the values appear too high. Both methods also reconstruct the outer target voxels with higher  $\lambda$  values compared to the interior voxels. The median method does appear to reconstruct the

scenario better than the average method, but there is work left to do to improve the overall discriminatory power and to reproduce actual physical  $\lambda$  values.

## 5. Discussion, Future Direction, and Summary

In this article we report our work on two tomography algorithms for reconstructing images from the scattering of cosmic ray muons for Homeland security applications. We also discuss an efficient but approximate median computation technique that we have developed to make the *EM-reconstruction* algorithm using the median feasible.

Some of the future directions of this work are to develop an integrated algorithm that will combine the two reconstruction algorithms described here for better efficiency and accuracy. We will also develop an online *anytime-good* reconstruction algorithm that will run as the data collection is ongoing where the accuracy will continuously improve over time to the maximum possible limit. For homeland security purposes such an algorithm should have a high practical value, where resource consumption is very important and cargo interrogation time is of the essence. Finally, we will run our experiments with more complex real life scenarios. We are also waiting for the availability of actual noisy experimental data [4] rather than using somewhat pure simulation data, to test the algorithms.

**Acknowledgement.** We acknowledge support from the U.S. Department of Homeland Security (DHS) and some students. The views and conclusions contained in this document are those of the authors and should not be interpreted as necessarily representing the official policies, either expressed or implied, of the DHS.

## References

1. Agostinelli, S., and one hundred twenty nine others, (2003) "GEANT4 – a simulation toolkit," *Nucl. Instrum.Meth. A*, 506, 250-303.
2. Allison, J., Amako, K., Apostolakis, J., Araujo, H., Dubois, P., Asai M., and others (2006) "GEANT4 developments and applications," *IEEE Trans. Nuclear Sc.*, 53(1), 270-278.
3. Bethe, H. (1953) "Moliere's theory of multiple scattering," *Physical Review*, 89(6), 1256.
4. Hohlmann, M., Ford, P., Gnanvo, K., Helsby, J., Pena, D., Hoch, R., and Mitra, D. (2008) "GEANT4 Simulation of a Cosmic Ray Muon Tomography System with Micro-Pattern GasDetectors for the Detection of High-Z Materials," *Proc. SORMA WEST'08 Conf.*, Berkeley, CA, *Trans. Nuclear Science*, article in press.
5. Schultz, L. J., Blanpeid, G. S., Borozdin, N., Fraser, A. M., Hengartner, N. W., Klimenko, A.V., Morris, C. L., Orum, J. C., and Sossong, M. J. (2007) "Statistical reconstruction for cosmic ray muon tomography," *IEEE Trans. Image Processing*, 16(8), pp. 1985-1993.
6. Sunday, D. (2006) "Distance between Lines and Segments with Their Closest Point of Approach." At: <http://geometrvalgorithms.com/Archive/algorithm0106/algorithm0106.htm>
7. Verdi, Y., Shepp, L. A., and Kaufman, L. (1985) "A statistical model for positron emission tomography." *I. Of American Statistical Association*, 80(389), 8-20.
8. Wright D., and others from the Cosmic-ray Physics Team at the Lawrence Livermore National Laboratory (2006) "Monte Carlo Simulation of Proton-induced Cosmic-ray Cascades in the Atmosphere," Lawrence Livermore National Lab., CA, *Tech. Rep. LA-UR-06-8497*.
10. C. Hagmann, D. Lange, and D. Wright "Cosmic-ray shower generator (CRY) for Monte Carlo transport codes," *2007 Proc. IEEE Nucl. Sci. Symp.*, Honolulu, HI, 2, 1143-1146.